Journal for Technology of Plasticity, Vol. 33 (2008), Number 1-2

FRICTION MODELS COMPARISON IN FINITE VOLUME METHOD SIMULATION OF BULK METAL FORMING TECHNOLOGIES

Hazim Bašić

Faculty of Mechanical Engineering, University of Sarajevo, Bosnia & Herzegovina

ABSTRACT

In this paper, the finite volume method (FVM) is used to calculate process parameters during extrusion of metals. FVM is applied on two-dimensional orthogonal grids and collocated variable arrangement. The application of the FVM is done in case of solving the plastic flow during extrusion processes with different boundary conditions. The method of involving of the most frequently used friction models, Coulomb's friction and constant friction law into the finite volume method algorithm is presented. The Eulerian description of motion to analyze of the metal flow is used. The obtained numerical results are in agreement with the theoretical considerations.

Key words*: Finite Volume Method, Extrusion, Friction modelling, Coulomb's friction, Constant friction law.*

1. INTRODUCTION

Friction is one of the most important problems in metal forming processes. It is a complex and hardly understood and controlled phenomenon. Due to the high pressures and temperatures, surface quality and lubrication properties, it is extremely difficult to perform the friction value and its influence on considered metal forming technology. Consequently, most information on friction phenomena is obtained by studying the workpiece surface after metal forming. These studies render some insight into the mechanisms that govern friction but do not supply sufficient information to specify the constitutive relations that can be applied to model friction in a forming analysis [1,2,13-15].

Therefore, the different friction laws are developed in order to describe the friction influence on the plastic metal flow during metal forming processes [9,11,14]. In this paper, the Coulomb's and the constant friction law are compared in the FVM algorithm for extrusion process simulation.

2. MATHEMATICAL MODEL

The most popular method used for simulation of the bulk metal forming processes is finite element method (FEM) [2,11,12,14]. But extrusion technologies are metal forming processes with severe and large plastic deformation. If the FEM is used to simulate extrusion process, mesh always distorts quickly and frequent remeshing is needed. In this paper, finite volume method (FVM) based on the Eulerian mesh is used to calculate relevant parameters of extrusion process. The finite volume method has dominated computational fluid dynamics for many years and has recently emerged as a viable numerical method for stress analysis in solid structures [6,7].

The process of cold extrusion can be described by flow formulation, which uses the velocity as dependent variables and governed by the following momentum and mass balance equations:

$$\int_S \rho u_i u_j n_j dS - \int_S \sigma_{ij} n_j dS = 0 , \tag{1}$$

$$\int_S \rho u_i n_j dS = 0 , \tag{2}$$

which are valid for an arbitrary part of continuum of the volume V bounded by the surface S, with surface vector n_j (j = 1, 2, 3) pointing outwards. In equations (1) and (2) ρ represents the density, u_i (i = 1, 2, 3) is the velocity vector and σ_{ij} (i = 1, 2, 3; j = 1, 2, 3) is the stress tensor.

In the simulation of extrusion processes, it is common to use a rigid-(visco)-plastic constitutive model to describe the material behavior and thus neglect the elastic properties of material. The reason for this is that the elastic deformations are small compared to the very large plastic deformations that occur during the process. For the relation between the stress tensor and the strain-rate tensor, the Levy-Mises equations are used:

$$\sigma_{ij} = -p\delta_{ij} + 2\mu\dot{\varepsilon}_{ij} , \tag{3}$$

where $p = (1/3)\sigma_{ii}$ is the pressure, δ_{ij} is Kronecker symbol ($\delta_{ij} = 1$ if $i = j$ and $\delta_{ij} = 0$ otherwise), $\dot{\varepsilon}_{ij}$ is the strain rate tensor with components:

$$\dot{\varepsilon}_{ij} = \frac{1}{2}\left(\frac{\partial u_i}{\partial x_j} + \frac{\partial u_j}{\partial x_i} \right), \tag{4}$$

and the viscosity μ is defined as

$$\mu = \frac{1}{3}\frac{\bar{\sigma}}{\bar{\dot{\varepsilon}}} , \tag{5}$$

where $\bar{\sigma} = \sqrt{3/2\,(\sigma'_{ij}\sigma'_{ij})}$ is the effective stress and $\bar{\dot{\varepsilon}} = \sqrt{2/3\,(\dot{\varepsilon}_{ij}\dot{\varepsilon}_{ij})}$ is effective strain rate.

During the calculation procedures, it is possible to obtain the too small values of effective strain rate in equation (5). This may cause the numerical instability, and the limiting value of the effective strain-rate $\bar{\dot{\varepsilon}}_0$, under which the material is considered to be rigid, must be introduced into calculation. One suggestion for determination of $\bar{\dot{\varepsilon}}_0$ is given in [4,5,9,10].

To accomplish the numerical model, in addition to the governing and constitutive equations, the appropriate boundary conditions have to be specified at the boundaries of the solution domain. The boundary conditions can be of Dirichlet (velocity prescribed, e.g. ram speed), or Neumann (e.g. zero gradient of velocity in extrusion direction on the die exit) type.

3. NUMERICAL METHOD

3.1. Finite volume discretisation

All numerical methods consist of transforming the governing equations into a system of (non-linear) algebraic equation, with subsets of these approximating each conservation equation. In order to achieve this the time, the space and the equations have to be discretised. The discretisaton procedure of equations (1) and (2) by employing a finite volume method is in detail described by Demirdžić and Muzaferija [7] and Ferziger and Peric [8]. The spatial domain is discretised into a finite number of contiguous arbitrarily shaped control volumes (CV) of volume V bounded by cell faces S_j, with computational nodes placed in the centre of each CV.

The boundary nodes, necessary for the specification of boundary conditions, are located in the centre of boundary cell faces, Figure 1.

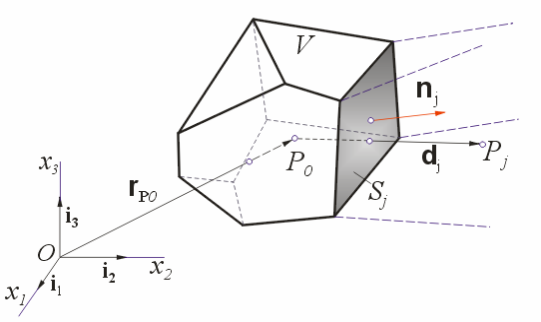

Figure 1 - Control volume of an arbitrary polyhedral shape

After introducing the constitutive relation (3), into equation for momentum balance (1) and integration over whole CV, the discretised equation for one CV is obtained:

$$\sum_{j=1}^{n}\int_{S_j}\rho u_i u_j n_j dS-\sum_{j=1}^{n}\int_{S_j}\mu\ \text{grad}\,u_i n_j dS=\sum_{j=1}^{n}\int_{S_j}\left\{\left[\mu(\text{grad}\,u_i)^T+p\mathbf{I}\right]\cdot\mathbf{i}_i\right\}n_j dS\quad(i=1,2,3)\qquad(6)$$

where n is the number of cells which share cell-faces with cell P_0, (i=1,2,3) are the Cartesian velocity vector components and $\mathbf{i}_i$ (i = 1,2,3) are the Cartesian base vectors.

The equation (6) has three distinct parts: convection and diffusion on the left hand side, and source term on the right hand side. The source term consists of terms coming from the stress tensor that are not contained in the diffusion term on the left hand side.
This equation is exact, i.e. no approximation has been introduced so far. However, in order to evaluate integrals in the above equation, a way of calculating integrals and a distribution of dependent variable u_i and physical properties of material in space have to be assumed.
The integrals in the discretised equation (6) are approximated by using the mid-point formula.
The gradients in equation (6) are calculated by assuming a linear spatial variation of dependent variables [5]. In this way equation (6) becomes a non-linear algebraic equation for each CV, which links the values of v_i at cell P_0 and its n nearest neighbors cells P_j:

$$a_{u_i 0} u_{iP_0} - \sum_{j=1}^{n} a_{u_i\, k} u_{iP_j} = b_{u_i} \,. \tag{7}$$

The coefficient matrix obtained by this procedure is diagonally dominant and sparse with a number of non-zero elements in each raw equal to the number of nearest neighbours n.

3.2. Solution procedure

After discretisation, a set of $4N$ non-linear coupled algebraic equations of the form (7) with $4N$ unknowns (tree components of velocity vector and pressure) is obtained for the solution domain consisting of N CVs. For the start of calculation, all dependent variables are given the corresponding initial values. Then the boundary conditions are applied. The equations are linearised and de-coupled by assuming that the coefficients and source terms are known and are obtained from the currently available values.
First, linearised momentum equations are solved, by using a conjugate gradient linear equations solver [7]. Then, the pressure-correction equation is solved and the calculated values are used to correct mass fluxes, velocity components and pressure. Finally the coefficient and source terms are updated and the procedure is repeated until a converged solution is obtained.
The pressure featuring in the source term of the discretised momentum equation is unknown and an independent use of the continuity equation (2) is not made yet. The pressure does not feature explicitly in continuity equation, therefore, some means for coupling the momentum and continuity equation and determining the pressure field are required. This is achieved by employing the predictor-corrector procedure defined by the SIMPLE algorithm [7,8], which results in a system of linear algebraic equations for pressure correction that has the same form as equation (7).

3.3. Friction models

To model the friction, a variety of constitutive laws can be used to define the surface tractions that are exerted on a material when it is sliding along a surface. Usually, the tangential surface tractions τ_s is related to the size of the normal surface traction σ_{sn} and to the relative sliding velocity along the tooling $\left(\mathrm{v} - \mathrm{v}_{tool}\right)$. As a point of departure, a Norton-Hoff type law is considered which has the following form [11]:

$$\tau_s = -m\sigma_{sn}^{\alpha} \left\| \mathbf{v} - \mathbf{v}_{tool} \right\|^{\beta-1} \left(\mathbf{v} - \mathbf{v}_{tool} \right) \tag{8}$$

where m represents the friction coefficient, and α and β are additional constitutive parameters. Notice that for this law the dimension of m depends on the choice of α and β.

For metal forming processes the velocity of the tooling is given by:

$$\mathrm{v}_{tool} = \begin{cases} 0 & \forall \mathrm{x} \in \Gamma_{die} \cup \Gamma_{container} \\ \mathrm{v}_{ram} & \forall \mathrm{x} \in \Gamma_{ram} \end{cases} \tag{9}$$

where Γ represents the corresponding surface area.

For the particular values of the parameters α and β, the following special friction laws are obtained:

- $\alpha = 0, \ \beta = 1$ - the Norton friction law,
- $\alpha = 0, \ \beta = 0$ - the constant friction law,
- $\alpha = 1, \ \beta = 0$ - the Coulomb's friction law.

In metal forming analysis, all of these laws have been used to model friction. However, in some technologies, like extrusion practice, it has been observed that locally increasing the length of the bearings above a certain value, does not further improve the balance of the extruded. This suggests that towards the exit of the bearing the frictional traction decreases and even vanishes for large bearing lengths. This trend cannot be captured by adopting the constant friction law.

Also, the Norton law is incapable of describing this behavior since it predicts that a particle that is sliding along the bearing will experience a frictional traction proportional to the sliding velocity. Since the velocity of a particle will not change significantly within the bearing, the Norton law suggests a nearly constant friction. Furthermore, there are indications that the sliding velocity has very little influence on the friction forces in metal-metal contact [11]. Therefore, the comparison between the Coulomb's and constant friction law is done.

3. 4. Numerical simulation of friction

For the frictional models comparison, the finite volume method, originally developed for the fluid flow and heat and mass transfer problems [8], is used in this paper. The tangential stress τ_b near to the cell faces with friction boundary conditions, Figure 2, is equal to product of viscosity and tangential velocity gradient in normal direction [3]:

$$\tau_b = \mu_b \left(\frac{\partial v_t}{\partial n} \right)_b = \begin{cases} mp_b & \text{- for Coulomb's friction law} \\ fk & \text{- for constant friction law} \end{cases} \tag{10}$$

where m and f are the friction coefficient and friction factor respectively, p_b is the pressure at the boundary node and k is the share yield stress.

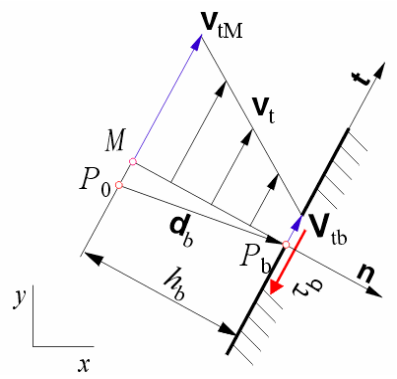

Figure 2 - Velocity profile near the contact wall

The tangential velocity on cell faces is extracted from equation (10):

$$v_{tb} = \begin{cases} v_{tM}\left(1 - m\dfrac{p_b}{\mu_b} h_b \dfrac{1}{|v_{tM}|}\right) & \text{- for Coulomb's friction law} \\ v_{tM}\left(1 - f\dfrac{k}{\mu_b} h_b \dfrac{1}{|v_{tM}|}\right) & \text{- for constant friction law} \end{cases} \tag{11}$$

where h_b is the normal distance between the calculation point M and boundary face, figure 2, and $\mathbf{v}_{tM}$ is obtained by linear interpolation from the values at points P_0 and P_k , where P_k are the neighbour control volumes. This boundary constrain is of Dirichlet (velocity prescribed) type.
The velocity profiles which correspond to the extreme values of contact friction (maximum friction factors and non-friction conditions) are given in Figure 3 and Figure 4.

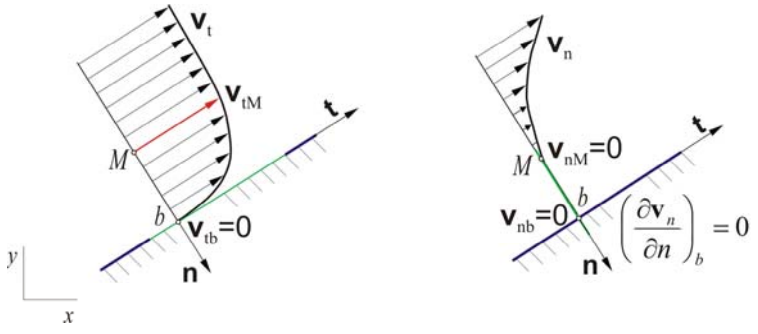

(a) (b)

Figure 3 - Velocity profiles near the contact wall for the case of maximum friction

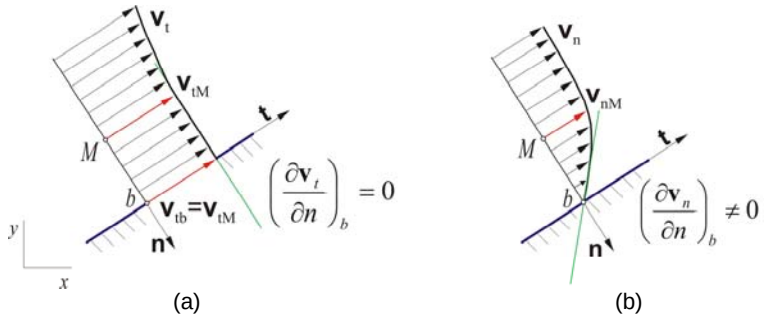

Figure 4 - Velocity profiles near the contact wall for the case of non-friction

The velocity profiles for extreme friction conditions given in Figure 3 and Figure 4 describe:

(a) the tangential velocity component profile for maximum friction (sticking wall),
(b) the normal velocity component profile for maximum friction,
(c) the tangential velocity component profiles for non-friction (slipping wall) and
(d) the normal velocity component profile for non-friction boundary condition.

4. THE NUMERICAL EXAMPLE

In this paper the constant friction and a Coulomb's friction models are analyzed in an example of plane strain forward extrusion through a flat faces die with the degree of deformation $\varepsilon = 50\%$. The prescribed workpiece yield stress is σ_Y=100 MPa, and a rigid-perfectly plastic model of material is used. The ram velocity is v_0=0,01 m/s. For the sake of simplicity, the friction boundary condition is prescribed only on the cylindrical part of the die.

The numerical mesh consisting of 900 control volumes together with prescribed boundary conditions is given in Figure 5. Due to the symmetry, only the half of the solution domain is used for calculation.

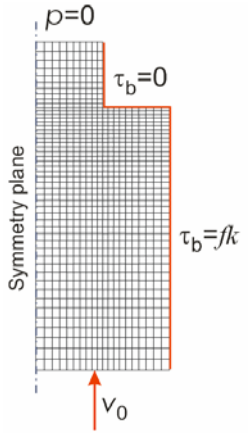

Figure 5 - The numerical mesh and boundary conditions

The obtained distributions of tangential stress component τ_{xy} for the constant friction law and different friction factors f are given in Figure 6.

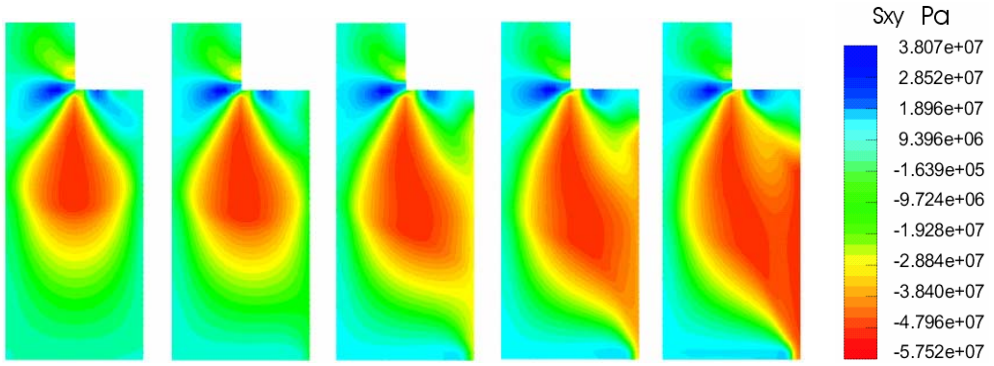

(a) $f = 0$ (b) $f = 0,2$ (c) $f = 0,5$ (d) $f = 0,7$ (e) $f = 1$

Figure 6 - Distribution of the tangential stress τ_{xy} for the constant friction law

One can see that the tangential stress on the die wall is systematically increased with the increasing of the friction factor. The case $f = 0$, Figure 6(a) corresponds to the sliding interface, while the case $f = 1$ represents the sticking wall (tangential stress on the die wall is equal to the shear yield stress $\tau_{xy} = k = 57,7$ Mpa), Figure 6(e).

The distribution of the velocity component in y-direction is given in Figure 7.

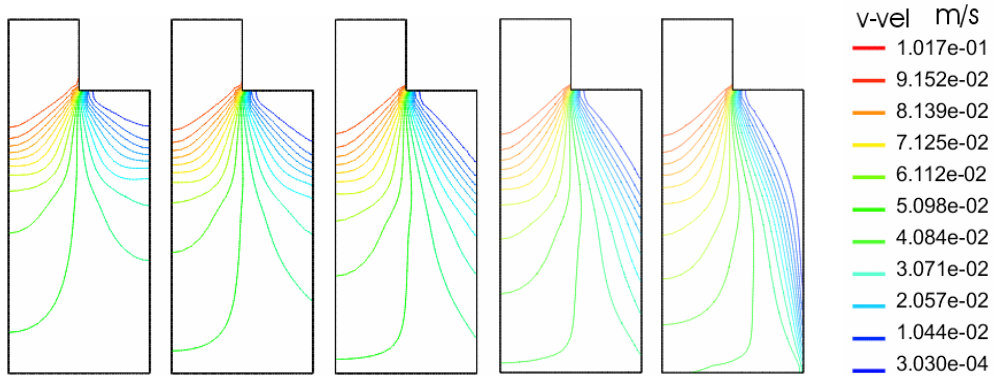

(a) $f = 0$ (b) $f = 0,2$ (c) $f = 0,5$ (d) $f = 0,7$ (e) $f = 1$

Figure 7 - The velocity distribution in flow direction

One can see that this velocity component near the wall become smaller with increasing the friction factor, and in extreme case $f = 1$ this velocity component is equal zero in the whole contact area, Figure 7(e) and 7(a) respectively.

The relation between the extrusion pressure and the friction factor/coefficient is given in Figure 8.

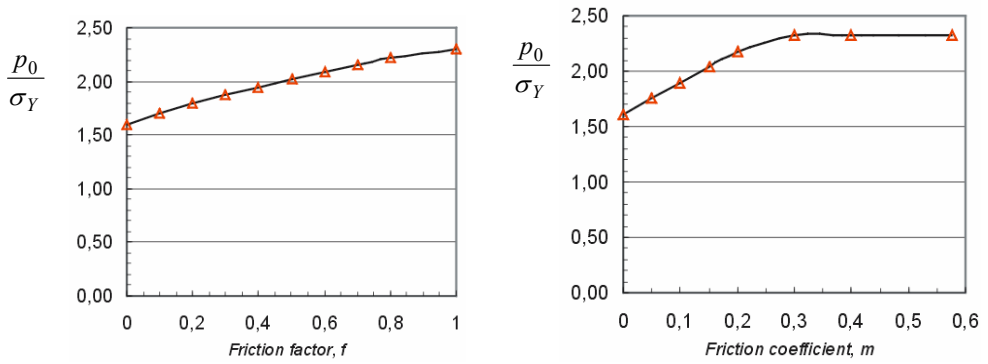

(a) (b)

Figure 8 - The relation between the extrusion pressure and friction factor/coefficient

One can see a uniform increasing of extrusion pressure in the case of constant friction law, Figure 8a. But, for the case of Coulomb's friction law the maximum extrusion pressure (corresponding to the sticking wall) is reached before, approximately for the friction coefficient $m = 0{,}3$. The further analyze shows that the value assigned to the Coulomb friction coefficient (or constant friction law) has a substantial influence on both the flow and the temperature fields of extrusion material.

5. CONCLUSION

The presented numerical method enable that in every point on the metal surface that is in contact with the tooling, the stress state and the velocity must satisfy the criteria that the frictional traction is opposed to the sliding velocity. Also, the stick and slip are mutually exclusive. FVM enables obtaining the distribution of velocity components and pressure field throughout the solution domain, from which the other important variables e.g. strain-rate and stress tensor components can be easily calculated. The main advantages of the FVM are its simplicity and an efficient use of computer resources (steaming out of the iterative segregated solution procedure). The calculated results are in good correlation with theoretical considerations [9,14] and experiments given in [12].

REFERENCES

[1]. Alexandrov, S., Mishuris, G., Miszuris, W., Sliwa, R.E.: On the dead-zone formation and limit analysis in axially symmetric extrusion, *Int. J. of Mechanical Sciences*, **43**, pp. 367-379, 2001.

[2]. Altan, T., *et al*.: Simulation of metal forming processes – applications and future trends, Advanced Technology of Plasticity, 6th International Conference–ICTP 99, Nurenberg, Vol. I, pp. 23-27, 1999.

[3]. Bašić, H., Demirdžić, I., Muzaferija, S.: Finite volume method for simulation of extrusion processes, *Int. J. for Numerical Methods in Engineering*; **62**, pp. 475–494, 2005
[4]. Bašić, H., Demirdžić, I., Muzaferija, S.: Analysis of plastic metal flow in extrusion technology using finite volume method, 3rd International Conference on Industrial Tools–ICIT 2001, Maribor-Rogaška Slatina, pp. 402-407, 2001.
[5]. Bašić H., *The application of the finite volume method on analysis of plastic metal flow in extrusion technologies*, Ph.D. Thesis, University of Sarajevo, 2002. (In Bosnian)
[6]. Demirdžić, I., Muzaferija, S.: Finite Volume Method for stress analysis in complex domains, *Int. J. for Numerical Methods in Engineering*, **37** (2), 3751-3766, 1994.
[7]. Demirdžić, I., Muzaferija, S.: Numerical Method for Coupled Fluid Flow, Heat Transfer and Stress Analysis Using Unstructured Moving Meshes with Cells of Arbitrary Topology, *Comput. Methods Appl. Mech. Engrg.*, **125**, pp. 235-255, 1995.
[8]. Ferziger, J.H., Peric, M.: *Computational Methods for Fluid Dynamics*, Springer, 1990.
[9]. Kobayashi, S., Oh, S., Altan, T.: *Metal Forming and the Finite Element Method*, Oxford University press, Oxford, 1989.
[10]. Lou, S., Zhao, G., Wang, R., Wu, X.: Modeling of aluminum alloy profile extrusion process using finite volume method, *J. of Materials Processing Technology*, **206**, 481-490, 2008.
[11]. Rens B.J.E., *Finite Element Simulation of the Aluminum Extrusion Process*, Ph.D. Thesis, University of Eindhoven, 1999.
[12]. Segal, V.M., Makušok, E.M., Reznikov, V.I.: *Isledovanie plastičeskogo formoizmenenija metalov metodom Muara,* Metalurgija, Moskva, 1974.
[13]. Qin, Y., Balendra, R.: Optimisation of the lubrication for the extrusion of solid and tubular components by injection forging, *J. of Materials Processing Technology*, **135**, pp. 219–227, 2003.
[14]. Wagoner R.H., Chenot J.L., *Fundamentals of Metal Forming,* John Wiley & Sons, New York, 1997.
[15]. Yanga, H., Penga, Y., Ruana, X., Liub, M.: A finite element model for hydrodynamic lubrication of cold extrusion with frictional boundary condition, *J. of Materials Processing Technology*, **161**, pp. 440–444, 2005.

KOMPARACIJA MODELA TRENJA KOD SIMULACIJE PROCESA ZAPREMINSKOG OBLIKOVANJA METALA PRIMJENOM METODE KONAČNIH VOLUMENA

Hazim Bašić

Univerzitet u Sarajevu, Mašinski fakultet Sarajevo, Vilsonovo šetalište 9, 71000 Sarajevo, Bosna I Hercegovina

REZIME

U radu je ukratko opisan matematički model na kojem se temelji primjena metode konačnih volumena za simulaciju procesa zapreminskog oblikovanja metala. Metoda je korištena na primjerima dvodimenzionalnih ortogonalnih domena kod kojih su računske tačke locirane u centrima kontrolnih volumena. Primjeri primjene odnose se na procese istosmjernog istiskivanja koji su tretirani kao kvazistacionarni uz različite kontaktne uslove. U radu je detaljno opisan pristup definisanja trenja na graničnim površinama. Ovaj pristup se temelji na činjenci da u izrazu za tangencijalni napon na graničnoj površini figurišu koeficijent trenja i gradijenti brzine. Tangencijalna komponenta brzina koja se dobije iz ovog izraza se zadaje kao granični uslov u kojem figuriše koeficijent trenja. Upoređivani su najčešće korišteni modeli trenja: Kulonov i zakon konstantnog trenja. Predloženi načini zadavanja trenja daju rezultate koji su u skladu s teorijski očekivanim vrijednostima (porast tangencijalnog napona na graničnoj površini od 0 za idealne kontaktne uslove do k za slučaj maksimalnog trenja kod kojeg je tangencijalna komponenta brzine jednaka nuli – lijepljenje materijala za stijenku matrice).

***Ključne reči**: Metoda konačnih zapremina, Istiskivanje, Modeliranje trenja, Kulonovo trenje, Kontaktno trenje.*